

# Analyst

Accepted Manuscript



This is an *Accepted Manuscript*, which has been through the Royal Society of Chemistry peer review process and has been accepted for publication.

*Accepted Manuscripts* are published online shortly after acceptance, before technical editing, formatting and proof reading. Using this free service, authors can make their results available to the community, in citable form, before we publish the edited article. We will replace this *Accepted Manuscript* with the edited and formatted *Advance Article* as soon as it is available.

You can find more information about *Accepted Manuscripts* in the [Information for Authors](#).

Please note that technical editing may introduce minor changes to the text and/or graphics, which may alter content. The journal's standard [Terms & Conditions](#) and the [Ethical guidelines](#) still apply. In no event shall the Royal Society of Chemistry be held responsible for any errors or omissions in this *Accepted Manuscript* or any consequences arising from the use of any information it contains.

# Recapitulation of *in vivo*-like Neutrophil Transendothelial Migration using a Microfluidic Platform

*Xiaojie Wu, Molly A. Newbold and Christy L. Haynes\**

Department of Chemistry, University of Minnesota, 207 Pleasant Street SE, Minneapolis,  
Minnesota, 55455, United States

\* To whom correspondence should be addressed

E-mail [chaynes@umn.edu](mailto:chaynes@umn.edu), Tel. +16126261096

## Abstract

Neutrophil transendothelial migration (TEM) is an essential physiological process that regulates the recruitment of neutrophils in response to inflammatory signals. Herein, a versatile hydrogel scaffold is embedded in a microfluidic platform that supports an endothelial cell layer cultured in the vertical direction and highly stable chemical gradients; this construct is employed to mimic the *in vivo* neutrophil TEM process. We found that the number of neutrophils migrating across the endothelial cell layer is dependent on the presented chemoattractant concentration and the spatial profile of the chemical gradient. Endothelial cells play a critical role in neutrophil TEM by promoting neutrophil morphological changes as well as expressing surface receptor molecules that are indispensable for inducing neutrophil attachment and migration. Furthermore, the microfluidic device also supports competing chemoattractant gradients to facilitate

1  
2  
3  
4 neutrophil TEM studies in complex microenvironments that more accurately model the *in*  
5  
6  
7 *vivo* system than simplified microenvironments without endothelial cells. This work  
8  
9  
10 demonstrates that combinations of any two different chemoattractants induce more  
11  
12 significant neutrophil migration than a single chemoattractant in the same total amount,  
13  
14 indicating synergistic effects between distinct chemoattractants. The *in vitro*  
15  
16 reconstitution of neutrophil TEM successfully translates planar neutrophil movement into  
17  
18 *in vivo*-like neutrophil recruitment and accelerates understanding of cellular interactions  
19  
20  
21 between neutrophils and endothelial cells within the complicated physiological milieu.  
22  
23  
24  
25  
26  
27  
28  
29  
30  
31  
32  
33  
34  
35  
36  
37  
38  
39  
40  
41  
42  
43  
44  
45  
46  
47  
48  
49  
50  
51  
52  
53  
54  
55  
56  
57  
58  
59  
60

## INTRODUCTION

As the most abundant white blood cell type, neutrophils function as the primary immune cells in various relevant diseases and recruit to the sites of infection through the endothelial cell layer in response to the physiological signals generated from invading microorganisms or local macrophages.<sup>1,2</sup> Neutrophil transendothelial migration (TEM) is a key multi-step process involved in inflammation since the activation of endothelial cells enables the capture of bypassing neutrophils and triggers the subsequent neutrophil inflammatory responses.<sup>3,4</sup> The highly orchestrated interactions between endothelial cells and neutrophils include the initial neutrophil rolling on endothelium, firm adhesion mediated by receptor molecules on cell surfaces, transcellular or paracellular extravasation, and final migration towards the inflammation locus.<sup>1,5,6</sup> Investigation of the neutrophil TEM process will shed light on the detailed mechanisms of cellular interactions between neutrophils and endothelial cells, also accelerating fundamental understanding of pathogenesis in neutrophil-related diseases.

Various traditional methods, such as the Boyden chamber<sup>7,8</sup> and transwell assays,<sup>9</sup> have been employed to recapitulate the *in vivo* leukocyte TEM processes; however, these approaches are not able to accurately represent the characteristics based on two main limitations: (1) conventional methods cannot achieve stable long-lasting chemical gradients to support the quantitation of neutrophil TEM and (2) these methods build up endothelial cell layers on a two-dimensional (2D) substrate that only facilitates neutrophil

1  
2  
3  
4 TEM observation through the basement membrane while ignoring the recruitment in  
5  
6 other directions. The chemical gradients generated by the chamber-based assays rely on  
7  
8 the free diffusion of molecules between two separated chambers such that the shapes of  
9  
10 gradients decay quickly and the results of neutrophil TEM cannot be interpreted in a  
11  
12 quantitative and controllable fashion. In addition, the upright filter membrane set up for  
13  
14 endothelial cell layer culture cannot reflect the whole picture of neutrophil TEM in  
15  
16 different directions and introduces the contribution of gravity into neutrophil TEM,  
17  
18 inspiring consideration of an improved platform to study the mechanisms of neutrophil  
19  
20 migratory behaviors.  
21  
22  
23  
24  
25  
26

27  
28  
29 Microfluidic technology, devices that allow the manipulation of small volume fluids in  
30  
31 microchannels,<sup>10</sup> is promising for recapitulation of the *in vivo* neutrophil TEM process,  
32  
33 especially with the inclusion of three-dimensional (3D) hydrogel matrices.<sup>11-14</sup> The  
34  
35 compact fibrous hydrogel structure, combined with the small dimensions of microfluidic  
36  
37 devices, facilitate the creation of predictable, reproducible, and long-term stable chemical  
38  
39 gradients with high spatiotemporal resolution so that the neutrophil TEM process can be  
40  
41 characterized in a real-time and quantitative manner. More importantly, the inclusion of  
42  
43 hydrogel materials not only provides mechanical support for the growth of an endothelial  
44  
45 cell layer in the perpendicular direction, but also successfully models extracellular matrix  
46  
47 (ECM) with realistic biophysical properties. With these efforts, a highly robust and  
48  
49 accurate microfluidic model can be developed to study the neutrophil TEM process.  
50  
51  
52  
53  
54  
55  
56  
57  
58  
59  
60

1  
2  
3  
4 Several previous examples have studied neutrophil migration through the endothelial cell  
5 layer using microfluidic platforms,<sup>15-18</sup> but these efforts failed to account for the real  
6 configuration of blood vessels or the various cellular stimuli. One promising advantage of  
7 our device design compared to the existing microfluidic assays is the introduction of  
8 multiple chemical gradients in different directions relative to the endothelial cell layer. In  
9 an *in vivo* setting, the neutrophil TEM process occurring at one specific site is guided by an  
10 array of chemoattractants gradients in different directions released from various biological  
11 sources; however, the existing microfluidic assays cannot recapitulate this  
12 microenvironment and only characterize neutrophil TEM without the complexity of  
13 multiple chemical gradients. The goal of this work was to build on previous efforts to  
14 create a versatile microfluidic platform, more similar to the complex physiological milieu,  
15 to study the critical process of neutrophil TEM.  
16  
17  
18  
19  
20  
21  
22  
23  
24  
25  
26  
27  
28  
29  
30  
31  
32  
33  
34

35  
36 Chemoattractants are the signaling molecules responsible for inducing neutrophil  
37 migration and activating endothelial cells in the neutrophil TEM process.<sup>19,20</sup> Herein, we  
38 considered neutrophil TEM under the influence of three inflammatory chemoattractants:  
39 interleukin-8 (IL-8), N-formyl-methionyl-leucyl-phenylalanine (fMLP), and leukotriene  
40 B4 (LTB4). IL-8, one of the primary chemoattractants initiating *in vivo* neutrophil TEM,  
41 is known to enhance cell adherence to matrix proteins, endothelium and tissues to  
42 promote cell recruitment.<sup>21</sup> Similar to IL-8, LTB4 is another type of host-derived  
43 chemoattractant that is known to induce cell adhesion, activation, and formation of  
44 reactive oxygen species.<sup>22,23</sup> On the contrary, fMLP is a formylated short peptide of  
45  
46  
47  
48  
49  
50  
51  
52  
53  
54  
55  
56  
57  
58  
59  
60

1  
2  
3  
4 bacterial origin and functions as an intense chemoattractant for several cell types.<sup>24</sup> As  
5  
6 mentioned above, the introduction of various chemical gradients within our microfluidic  
7  
8 device is able to establish the hierarchy of these three chemoattractants through  
9  
10 developing competing chemical gradients in two opposing symmetric channels, which  
11  
12 enables the mechanistic investigation of neutrophil migratory signaling cascades during  
13  
14 decision-making process.  
15  
16  
17  
18

## 19 20 **EXPERIMENTAL SECTION**

### 21 22 **Device fabrication**

23  
24 Standard photolithography protocols were applied to fabricate microfluidic devices.  
25  
26 The design of the device was printed on a film (CAD/Art Service Inc., Bandon, OR) with  
27  
28 transparent channel patterns and a lightproof background. Through the exposure to UV  
29  
30 light, channel patterns were transferred onto a chrome photomask plate coated with  
31  
32 AZ1518 positive photoresist layer (Nanofilm, Westlake Village, CA), and then  
33  
34 cross-linked photoresist in the channels was removed by placing the photomask in 351  
35  
36 developer solution (Rohm and Hass Electronic Materials LLC, Marlborough, MA).  
37  
38 Then, the exposed chrome layer was etched down in the chrome etchant solution  
39  
40 (Cyantek Corporation, Fremont, CA). To remove the residual photoresist, the photomask  
41  
42 was immersed in piranha solution (1:1 volume ratio of 30% hydrogen peroxide and 99.9%  
43  
44 sulfuric acid, Avantor Performance Materials, Phillipsburg, NJ) and then washed using  
45  
46 deionized (DI) water. After the preparation of the photomask, the microfluidic device  
47  
48 mold was fabricated by spin-coating a 4-inch silicon wafer with 120- $\mu\text{m}$ -thick negative  
49  
50  
51  
52  
53  
54  
55  
56  
57  
58  
59  
60

1  
2  
3  
4 SU-8 50 photoresist (MicroChem, Newton, MA). The channel patterns were imprinted on  
5  
6 the SU-8 mold through the previously made photomask *via* UV exposure following an  
7  
8 initial baking step. The silicon wafer was placed in SU-8 developer (MicroChem, Newton,  
9  
10 MA) to remove the photoresist without exposure, and the channel patterns were left on  
11  
12 the mold. A 10:1 mass ratio mixture of Sylgard 184 silicone elastomer base and curing  
13  
14 agent (Ellsworth Adhesives, Germantown, WI) was poured on the SU-8 mold and kept on  
15  
16 a hot plate at 95 °C overnight. Medium channel reservoirs and gel chamber inlets were  
17  
18 punched at appropriate points in the polydimethylsiloxane (PDMS) layer using 3.5 mm  
19  
20 and 1 mm disposable biopsy punches (Integra Miltex, Plainsboro, NJ), respectively.  
21  
22 Finally, the PDMS layer was cut and then permanently attached to a glass slide by using  
23  
24 oxygen plasma for 10 seconds at 100 L/h oxygen flow rate and 100 W.  
25  
26  
27  
28  
29  
30  
31  
32

### 33 **Endothelial Cell Culture**

34  
35  
36 The human endothelial cell line hy926, a phenotype suitable for neutrophil-endothelial  
37  
38 cell interaction studies,<sup>16,25,26</sup> was purchased from American Type Culture Collection  
39  
40 (ATCC, Manassas, VA) and stored in liquid nitrogen storage container (MVE XC33/22,  
41  
42 Select Genetics, Washington, PA). Upon thawing, endothelial cells were dispensed into a  
43  
44 75 cm<sup>2</sup> flask containing 20 mL of Dulbecco's Modified Eagle Medium (DMEM, formula:  
45  
46 4mM L-glutamine, 4.5 g/L L-glucose, and 1.5 g/L sodium pyruvate, Gibco, Carlsbad, CA)  
47  
48 supplemented with 10% fetal bovine serum and 1% penicillin and streptomycin  
49  
50 (Sigma-Aldrich, St. Louis, MO). Cells were fed every other day and, when necessary,  
51  
52 cells were detached using 1× trypsin solution (Sigma-Aldrich, St. Louis, MO) for device  
53  
54  
55  
56  
57  
58  
59  
60



1  
2  
3  
4 injection. Endothelial cells were only used between the third and tenth passages.  
5  
6

### 7 **Device Preparation**

8  
9 First, microfluidic devices were filled with 30  $\mu\text{L}$  of 1 mg/mL Poly-D-Lysine (PDL)  
10 solution (Sigma-Aldrich, St. Louis, MO) and incubated for 4 h under 5%  $\text{CO}_2$  at 37  $^\circ\text{C}$ .  
11  
12 After the completion of surface coating, devices were rinsed with 30  $\mu\text{L}$  of sterilized  
13 Milli-Q water (Millipore, Billerica, MA) twice to remove excess PDL solution that may  
14  
15 cause damage to cells. Prior to introducing gel, devices were placed in the oven at 65  $^\circ\text{C}$   
16  
17 for 24 to 48 h so that the hydrophobicity of devices was restored. Collagen type I gel  
18  
19 solution (BD Biosciences, San Jose, CA), one common hydrogel material used for  
20  
21 simulating extracellular matrix,<sup>12,15,27</sup> was diluted to a concentration of 2 mg/mL and  
22  
23 injected into the gel chamber through the gel inlet. To avoid the evaporation of gel  
24  
25 solution, all the devices were kept in humid pipette boxes after the gel injection and a  
26  
27 thermally induced polymerization was carried out under 5%  $\text{CO}_2$  at 37  $^\circ\text{C}$  for 30 min. The  
28  
29 porous fiber structure of the resulting collagen gel was visualized using a scanning  
30  
31 electron microscope (SEM, see the details in Supporting Information). After the gel  
32  
33 polymerization, 20  $\mu\text{L}$  of cell culture medium was forcibly injected into each channel of  
34  
35 the microfluidic device, and the medium in all six reservoirs was aspirated before loading  
36  
37 endothelial cells. Endothelial cells were trypsinized and re-suspended in the cell culture  
38  
39 medium for a proper density ( $1.5 - 2 \times 10^6$  cells/mL), and then 20  $\mu\text{L}$  of endothelial cells  
40  
41 were seeded into a reservoir of the bottom channel to enable the cell layer to attach on the  
42  
43 side wall of gel because of the pressure difference between the bottom channel and side  
44  
45  
46  
47  
48  
49  
50  
51  
52  
53  
54  
55  
56  
57  
58  
59  
60

1  
2  
3  
4 channels. Following an initial incubation under 5% CO<sub>2</sub> at 37 °C for 30 min, the medium  
5  
6 was aspirated from the bottom reservoirs, and 30 μL of fresh medium was added in each  
7  
8 reservoir. Finally, all the devices were placed in the CO<sub>2</sub> incubator (New Brunswick  
9  
10 Scientific, Edison, NJ) overnight for confluent growth of the endothelial cell layer. For  
11  
12 the conditions without an endothelial cell layer, the same procedure was used except for  
13  
14 the addition of endothelial cells in the devices. The details about endothelial  
15  
16 cell-conditioned medium experiments are included in Supporting Information.  
17  
18  
19  
20  
21

### 22 **Neutrophil Isolation**

23  
24 Ethylenediaminetetraacetic acid (EDTA)-anticoagulated freshly drawn human blood  
25  
26 samples were prepared by Memorial Blood Center (St. Paul, MN) according to IRB  
27  
28 protocol E&I ID no. 07809. Samples were collected only from healthy donors following  
29  
30 the guidelines that meet the standards of the Food and Drug Administration. Immediately  
31  
32 after blood samples were collected, neutrophils were separated and purified using a  
33  
34 previously reported isolation protocol.<sup>28</sup> Carefully, 5 mL of blood sample was layered on  
35  
36 the same volume of mono-poly resolving medium (Fisher Scientific, Waltham, MA) and  
37  
38 promptly centrifuged to obtain a distinct neutrophil band. Neutrophils were washed using  
39  
40 red blood cell lysis buffer (Miltenyi Biotec Inc., Auburn, CA) several times (2.5 mL for  
41  
42 each time) until only white cells were left at the bottom of centrifuge tube. The final  
43  
44 neutrophil pellet was re-suspended in Hank's buffered salt solution (HBSS, Fisher  
45  
46 Scientific, Waltham, MA) containing 2% human serum albumin (HSA, Sigma-Aldrich, St.  
47  
48 Louis, MO) at a cell density between 4 - 5 × 10<sup>6</sup> cells/mL.  
49  
50  
51  
52  
53  
54  
55  
56  
57  
58  
59  
60

## Neutrophil Transendothelial Migration Experiments

Before introducing neutrophils into the device, the medium in each of the reservoirs terminating the bottom and left channels was replaced with 30  $\mu\text{L}$  of HBSS buffer while medium in each reservoir of the right channel was changed to 30  $\mu\text{L}$  of chemoattractant solution (IL-8 and fMLP, Sigma-Aldrich, St. Louis, MO; LTB<sub>4</sub>, Cayman Chemical, Ann Arbor, MI). Different chemoattractant solutions were placed in the two opposing side channels for competing gradient conditions, and HBSS buffer was placed in the both channels in the chemoattractant-free condition. It took approximately 2 h to achieve completely stable diffusion of chemoattractant molecules in the gel scaffold. Then, 5  $\mu\text{L}$  of neutrophils of the desired density were added into the bottom channel of the device. Neutrophil TEM was monitored using MetaMorph ver. 7.7.5 imaging software (images recorded every other hour for 5 h) on an inverted microscope equipped with a 10 $\times$  objective (Nikon, Melville, NY) and a CCD camera (QuantEM, Photometrics, Tucson, AZ). Data from neutrophils collected from three different donors were measured in each condition.

## RESULTS AND DISCUSSION

### Characterization of Neutrophil TEM System

The microfluidic device consists of two side channels, one bottom channel and the central gel chamber that separates these three channels (Fig. 1(a) and (b)). In our design, endothelial cells attached to the side wall of collagen gel are activated by the chemoattractants originating from the side channels; meanwhile, neutrophils in the

1  
2  
3  
4 bottom channel received the biological signals from endothelial cells and complete the  
5  
6  
7 TEM process along the direction of the chemical gradients. The prerequisite for  
8  
9  
10 establishing chemical gradients in the collagen gel is the stable diffusion of  
11  
12 chemoattractant molecules between two symmetrical side channels. Due to the solid 3D  
13  
14 cross-linked network of collagen gel, molecular diffusion is confined at a slow and  
15  
16 uniform rate that promotes the long-term stabilization of chemical gradient. To verify the  
17  
18 diffusion characteristics of chemoattractant molecules, theoretical simulation and  
19  
20 experimental fluorescence imaging have been employed to observe the chemical gradient  
21  
22 in the collagen gel. The simulation result (Fig. 1(d)) using finite element method software  
23  
24 COMSOL 4.3b reveals that the chemical gradient across the center line in the gel  
25  
26 chamber produced by 50 ng/mL fMLP solution is linear and stable from 1 h to 10 h  
27  
28 diffusion (Fig. 1(c) shows the diffusion of fMLP molecules at 5 h), which is suitable for  
29  
30 examining neutrophil TEM with reproducible spatiotemporal resolution. Also, the  
31  
32 chemical gradient was visualized at different time points by placing Rhodamine 6G  
33  
34 solution in the right side channel and monitoring the fluorescence gradient across the  
35  
36 center line in the gel chamber; this experiment demonstrated that a stable fluorescent  
37  
38 gradient can be achieved after 2 h diffusion, and there is no apparent decay until 10 h (Fig.  
39  
40 1(e)). The profiles of chemical gradients are similar between those apparent in the  
41  
42 COMSOL simulation and the empirical fluorescence imaging results, but it takes longer  
43  
44 than expected (2 h vs. 1 h as predicted by COMSOL) to reach stable diffusion for  
45  
46 fluorescence imaging; as a result, 2 h was used as the wait time for gradient formation  
47  
48  
49  
50  
51  
52  
53  
54  
55  
56  
57  
58  
59  
60

1  
2  
3  
4 before neutrophil injection. Since the diffusion coefficient is directly relevant to the  
5  
6 molecular weight, the established Rhodamine 6G (~479 Da) gradient will be very similar  
7  
8 to fMLP (~437 Da) and LTB4 (~340 Da) conditions. Although IL-8 has a much higher  
9  
10 molecular weight (~ 8.4 kDa) than the other two chemoattractants, this difference is  
11  
12 likely compromised in the highly compact gel structure such that all of the  
13  
14 chemoattractants have similar diffusive behaviors.<sup>15</sup> In addition to examining the center  
15  
16 line of gel chamber, we found that the fluorescence gradient becomes steady after 2 h at  
17  
18 other positions, including the gel-endothelial cell interface and the vertical direction  
19  
20 across cell layer that characterizes the gradient from top to bottom part (Fig. S1),  
21  
22 suggesting that gradients in various parts of the microfluidic devices reach stabilization  
23  
24 after the first 2 h and can be maintained for a long time. Furthermore, the results of  
25  
26 confocal and dark-field imaging confirm the confluency of the whole endothelial cell  
27  
28 layer structure on the side wall of gel scaffold (Fig. 1(f) and S2) and the confocal images  
29  
30 of three different devices clearly indicate the good reproducibility of cell layer  
31  
32 configuration from device to device (Fig. S3). The permeability of the endothelial cell  
33  
34 layer was measured by analyzing fluorescence images of the device after 2 h diffusion of  
35  
36 fluorescein isothiocyanate (FITC)-dextran solution across the endothelial cell layer from  
37  
38 the bottom channel to the gel scaffold (Fig. S4); the measured permeability was  $5.73 \times$   
39  
40  $10^{-7}$  m/s, a value similar to those reported in the other *in vitro* systems with a  
41  
42 non-permeable endothelial cell layer,<sup>15,29</sup> indicating a good seal between the endothelial  
43  
44 cell layer and PDMS substrate. Together, these device characterizations suggest that this  
45  
46  
47  
48  
49  
50  
51  
52  
53  
54  
55  
56  
57  
58  
59  
60

1  
2  
3  
4 microfluidic platform will be a good model for the *in vivo* neutrophil TEM system.  
5  
6

### 7 **Neutrophil TEM Under Single Chemoattractant Gradients**

8

9  
10 With a well-characterized device, the neutrophil TEM process was first examined under  
11  
12 single chemoattractant gradients. For each chemoattractant, three different concentrations  
13  
14 (10 ng/mL, 20 ng/mL, and 50 ng/mL) were employed to build up chemical gradients  
15  
16 from the right channel to the left channel; neutrophil migration in the gel chamber was  
17  
18 monitored every other hour after neutrophil injection into the device. The images at 5 h  
19  
20 (Fig. 2(a) - (c)) clearly show that a number of neutrophils migrate into the gel region  
21  
22 across the endothelial cell layer in each condition. To quantify the results of neutrophil  
23  
24 TEM, we simply counted the number of cells in different regions of the gel chamber (Fig.  
25  
26 3) with linear and continuous gradients so that the effects of localized chemoattractant  
27  
28 concentrations on neutrophil polarization could be determined. The largest concentrations  
29  
30 (50 ng/mL) for all the chemoattractants (fMLP: 114 nM; LTB4: 147 nM; IL-8: 5.95 nM)  
31  
32 lead to significant differences between the neutrophils present in the left and right  
33  
34 portions of the device; however, there is no significant difference found with lower  
35  
36 chemoattractant concentrations (10 ng/mL and 20 ng/mL) except for 20 ng/mL IL-8 (Fig.  
37  
38 4). It is worth mentioning that different gel interface shapes caused by various surface  
39  
40 tensions do not lead to the considerable deviation in average values of three replicates  
41  
42 since the flat gradient shape in the vertical direction across the cell layer is not sensitive  
43  
44 to small changes in the gel interface position (Fig. S1(b)). Additionally, the arc-shaped  
45  
46 interfaces do not influence the number of neutrophils interacting with the endothelial cell  
47  
48  
49  
50  
51  
52  
53  
54  
55  
56  
57  
58  
59  
60

1  
2  
3  
4 layer due to the significant larger dimension of bottom channel for neutrophil injection.  
5  
6  
7 The amount of chemoattractants in each part of the gel chamber is proportional to the  
8  
9 total chemoattractant concentration presented in the side channel, so the concentration  
10  
11 differences between the left and right gel region become larger as the total  
12  
13 chemoattractant concentrations increase. Neutrophils sense a steeper gradient in the  
14  
15 condition of 50 ng/mL chemoattractant compared to the lower concentrations, and many  
16  
17 more neutrophils prefer moving towards the chemoattractant sources (i.e. the steeper  
18  
19 portion of the chemoattractant gradient) on the right side. On the contrary, no statistical  
20  
21 difference is observed between the cell numbers located in the top and bottom portion of  
22  
23 the gel-filled chamber for any of the three chemoattractants, even at the highest  
24  
25 concentrations (Fig. S5). The flat slope of the fluorescence gradient in the vertical  
26  
27 direction (Fig. S1(b)) suggests that chemoattractant molecules distribute evenly between  
28  
29 the top and bottom regions, and the small concentration difference is not enough to  
30  
31 induce significant neutrophil migration. To examine neutrophil TEM without chemical  
32  
33 gradients in the horizontal direction, 25 ng/mL of each chemoattractant was placed in  
34  
35 both side channels such that the average concentration is the same as the single chemical  
36  
37 gradient condition (50 ng/mL). The simulation results using fMLP as a model  
38  
39 chemoattractant indicate that the gradient profile is symmetric along the horizontal  
40  
41 direction in the “no gradient” condition while the gradient profiles in the vertical direction  
42  
43 are the same for single chemoattractant gradient and “no gradient” conditions, which  
44  
45 means these two conditions both have the steepest gradient in the perpendicular direction  
46  
47  
48  
49  
50  
51  
52  
53  
54  
55  
56  
57  
58  
59  
60

1  
2  
3  
4 and the same total amounts of chemoattractant molecules in the gel scaffold because of the  
5  
6 identical average concentration (Fig. S6). The neutrophil migration results reveal no  
7  
8 significant difference in cell numbers between the left and right device regions in the “no  
9  
10 gradient” condition and there are still not statistically more neutrophils moving into the top  
11  
12 device region (Fig. S7). Thus, we can conclude that the symmetric gradient profile  
13  
14 diminishes the polarization of neutrophil TEM in the horizontal direction, and the  
15  
16 migration of cells along the vertical direction is determined by the average concentration of  
17  
18 chemoattractants in the side channels. Based on the results above, this work reveals that  
19  
20 high chemoattractant concentrations with steep chemical gradients are able to cause  
21  
22 distinguishable neutrophil TEM processes, which is consistent with disease models where  
23  
24 excessive amounts of neutrophils accumulate around infection sites, likely induced by the  
25  
26 high level of chemoattractants in the context of diseases.  
27  
28  
29  
30  
31  
32  
33  
34  
35

### 36 **The Role of Endothelial Cell Layer in Neutrophil Transmigration**

37  
38 One interesting phenomenon revealed in this study is that neutrophils do not migrate into  
39  
40 the gel chamber without an endothelial cell layer in any of the presented conditions;  
41  
42 without the endothelial cell layer, neutrophils only gather at the interface between the gel  
43  
44 chamber and the bottom channel after 5 h migration (Fig. 2(d) - (f)). The collagen gel  
45  
46 with a small pore size (Fig. S8) functions as a physical barrier to prevent the infiltration  
47  
48 of neutrophils and endothelial cells into the gel and neutrophils must undergo  
49  
50 morphological changes before entering the gel due to the comparatively large diameter of  
51  
52 a single neutrophil ( $\sim 10 \mu\text{m}$ ). A morphological difference is clear between the spherical  
53  
54  
55  
56  
57  
58  
59  
60



1  
2  
3  
4 neutrophils without an endothelial cell layer and the stretched neutrophils that are moving  
5  
6 through the gel chamber in the presence of an endothelial cell layer (Fig. S9). To assess  
7  
8 the possibility that biological molecules secreted by the endothelial cells promote the  
9  
10 neutrophil morphological changes, all the molecules in the endothelial cell  
11  
12 conditioned-medium after overnight (~ 12 h) chemoattractant-activation were collected  
13  
14 and placed in the aforementioned microfluidic devices (see the details in Supporting  
15  
16 Information) without adding the actual endothelial cells. The timescale used herein is  
17  
18 suitable to maintain activity of the endothelial cell secreted species.<sup>30-32</sup> Neutrophils were  
19  
20 introduced as previously described, images were captured, and cells were counted. Even  
21  
22 in the presence of the endothelial cell-secreted soluble molecules, neutrophils stayed in  
23  
24 the bottom channel instead of penetrating into the collagen gel (Fig. S10), signifying that  
25  
26 the biological secretion alone is not strong enough to induce neutrophil deformation.  
27  
28 Some previous work<sup>33-35</sup> indicates that the mechanical interactions between neutrophils  
29  
30 and endothelia cells initiate the disruption of cell-cell junctions and enable neutrophils to  
31  
32 undergo morphological changes to complete the extravasation step. The biological  
33  
34 molecules regulating this process, such as intercellular adhesion molecule-1 (ICAM-1),  
35  
36 guanine exchange factor (GEF), and myosin light chain kinase (MLCK),<sup>33</sup> are either  
37  
38 intracellular species or molecules expressed on the surfaces of cells, and thus not secreted  
39  
40 as soluble factors into the free medium, meaning that secreted molecules cannot promote  
41  
42 neutrophil migration in the absence of the actual endothelial cell layer; however, more  
43  
44 experiments will be pursued in the future to further explore mechanical effects in a  
45  
46  
47  
48  
49  
50  
51  
52  
53  
54  
55  
56  
57  
58  
59  
60

1  
2  
3  
4 biologically relevant environment. In addition to inducing shape change in neutrophils,  
5  
6 another important role of endothelial cells in neutrophil TEM is to express surface  
7  
8 receptors for triggering neutrophil attachment. The result of chemoattractant-free control  
9  
10 conditions (Fig. S11 (a)) shows that no neutrophil attachment or migration is detected  
11  
12 without chemoattractant signals, even in the presence of an endothelial cell layer. To  
13  
14 examine the effects of chemoattractants on endothelial cell activation, the expression of  
15  
16 two major adhesion molecules known to regulate neutrophil-endothelial cell interaction,  
17  
18 p-selectin and intercellular adhesion molecule-1 (ICAM-1),<sup>5,36</sup> were visualized using  
19  
20 antibody fluorescence imaging (Fig. S11(b) and (c)). After the activation by 50 ng/mL of  
21  
22 IL-8 gradient (fMLP and LTB4 data not shown), endothelial cells display a much higher  
23  
24 level of adhesion molecules than the condition in the absence of chemoattractant,  
25  
26 suggesting that chemoattractant activation is the main driving force for receptor  
27  
28 expression and non-activated endothelial cells are not able to induce neutrophil TEM  
29  
30 process. Further evidence was obtained by examining neutrophil TEM under the same  
31  
32 IL-8 gradient but with the antibodies for adhesion molecules, and no neutrophil TEM was  
33  
34 detected after 5 h cell addition (Fig. S11(d)). Based on the observations above, the role of  
35  
36 endothelial cells in neutrophil TEM must: (1) promote the morphological changes of  
37  
38 neutrophils to enable cell extravasation into the ECM and (2) present the surface receptor  
39  
40 molecules for initiating neutrophil attachment and migration.  
41  
42  
43  
44  
45  
46  
47  
48  
49  
50  
51  
52  
53  
54

### 55 **Neutrophil TEM under Competing Chemoattractants Gradients**

56  
57 To examine neutrophil TEM under competing gradients, different types of  
58  
59  
60

1  
2  
3  
4 chemoattractants at 50 ng/mL were placed in two opposing side channels. The results of  
5  
6  
7 single chemoattractant gradient conditions reveal that 50 ng/mL of each chemoattractant  
8  
9  
10 is capable of inducing similar numbers of neutrophils to transmigrate across the  
11  
12 endothelial cell layer, so 50 ng/mL was used as the concentration for developing  
13  
14 competing gradients. Of the three chemoattractants pairs, significant differences in cell  
15  
16 numbers between the left and right regions of the gel chamber, thus indicating a  
17  
18 neutrophil preference for one chemoattractant or the other, are observed in the conditions  
19  
20 of fMLP vs. IL-8 and LTB4 vs. IL-8 (the former chemoattractant is in the left channel)  
21  
22 while there is no significant difference found in the condition of LTB4 vs. fMLP (Fig. 5).  
23  
24  
25 Statistically, more neutrophils migrate towards the other type of chemoattractant in  
26  
27 IL-8-containing competing gradients, which means both fMLP and LTB4 are dominant  
28  
29 chemoattractants over IL-8 during the neutrophil TEM process. The comparison between  
30  
31 LTB4 and fMLP indicates that these two chemoattractants have similar abilities to  
32  
33 mediate the polarization of neutrophil TEM. Considering the results above, the hierarchy  
34  
35 among these chemoattractants is  $fMLP = LTB4 > IL-8$ . Although neutrophil migration  
36  
37 under competing gradients has been studied in previous research using microfluidic  
38  
39 platforms,<sup>37-39</sup> these studies did not incorporate the endothelial cell layer into the devices,  
40  
41 and the hierarchy among multiple chemoattractants was only obtained in simplified  
42  
43 microenvironments. The hierarchy reported herein agrees with the previous conclusion  
44  
45 that the p38 mitogen-activated protein (MAP) pathway related to fMLP overwhelms the  
46  
47 phosphatidylinositol 3-kinase (PI3K) signaling pathway activated by IL-8.<sup>40,41</sup> As another  
48  
49  
50  
51  
52  
53  
54  
55  
56  
57  
58  
59  
60

1  
2  
3  
4 PI3K pathway-controlled chemoattractant, the competence of LTB<sub>4</sub> in attracting  
5  
6  
7 neutrophil migration is enhanced in the presence of the endothelial cell layer; better  
8  
9  
10 understanding of the molecular mechanisms behind this behavior will be the focus of  
11  
12 future work. Unlike the single chemoattractant gradients, all the competing gradients  
13  
14  
15 conditions demonstrate significant differences in the number of cells in the top and  
16  
17  
18 bottom regions of the gel chamber, confirming the observation that the increase in the  
19  
20 total amount of chemoattractants (from 50 ng/mL to 100 ng/mL) enables the production  
21  
22  
23 of steeper gradients and thus, statistically distinct neutrophil TEM.

### 24 25 **Synergistic Chemoattractant Effects on Neutrophil TEM**

26  
27  
28 In the conditions of single chemoattractant gradients, 50 ng/mL of each chemoattractant  
29  
30  
31 was not able to induce significant differences between the number of neutrophils  
32  
33  
34 migrating into the top and bottom portions of the gel-filled chamber due to the flat  
35  
36  
37 gradient shape in the vertical direction. The previous study suggested the cooperative  
38  
39  
40 interplay taking place between two different chemoattractants to promote neutrophil  
41  
42  
43 migratory responses.<sup>37</sup> With this neutrophil transendothelial migration model, we also  
44  
45  
46 hypothesized that various chemoattractants coexisting in the channel, at the same total  
47  
48  
49 chemoattractant concentration as the single chemoattractant gradients, would influence  
50  
51  
52 neutrophil TEM in the vertical direction. The mixture of any two chemoattractants, with  
53  
54  
55 25 ng/mL concentration for each one, was employed to replace single chemoattractant  
56  
57  
58 solution in this experiment. For all three conditions, significant differences are observed  
59  
60  
61 between the number of cells in the top and bottom portions of the chamber (Fig. 6),

1  
2  
3  
4 which means that these chemoattractants function through synergistic effects to mediate  
5  
6 the neutrophil TEM process. This is likely attributable to the fact that multiple  
7  
8 chemoattractants trigger downstream signaling pathways using different surface receptors  
9  
10 cooperatively, thus speeding up the responses of neutrophil migration. On the other hand,  
11  
12 a single chemoattractant only binds to the corresponding receptor in a competitive  
13  
14 manner that reduces the efficiency of initiating neutrophil TEM. In addition, the  
15  
16 combination of any two chemoattractants does not alter the chemoattractant concentration  
17  
18 gradients from right to left, and the significant differences between the number of cells in  
19  
20 the left and right portions of the chamber remain unchanged compared to the single  
21  
22 chemoattractant gradients. We also evaluated the synergistic effects within the competing  
23  
24 gradients by introducing 25 ng/mL of two different chemoattractants in the side channels  
25  
26 separately. Compared to integrating two chemoattractants in one side channel, competing  
27  
28 gradients provide a symmetric distribution of different chemoattractant molecules across  
29  
30 the gel chamber but maintain the same total amount of chemoattractants in the top and  
31  
32 bottom regions. All three competing gradients still indicate the synergistic effects in the  
33  
34 vertical direction compared to placing 25 ng/mL of the same chemoattractant in both side  
35  
36 channels (Fig. S7) while the hierarchy among these three chemoattractants is disrupted,  
37  
38 and the significant difference between the cell numbers in the left and right portions of  
39  
40 the chamber is only found in the LTB<sub>4</sub>-IL-8 pair (Fig. S12). Another interesting  
41  
42 discovery is that the total cell numbers completing transmigration across the endothelial  
43  
44 cell layer after 5 h observation is not statistically different for 25 ng/mL and 50 ng/mL  
45  
46  
47  
48  
49  
50  
51  
52  
53  
54  
55  
56  
57  
58  
59  
60

1  
2  
3  
4 competing gradients conditions although the total concentration of chemoattractants for  
5  
6  
7 50 ng/mL competing gradients is twice as that in 25 ng/mL competing gradients  
8  
9  
10 conditions. Further examination of adhesion molecule expression (p-selectin and ICAM-1)  
11  
12 reveals that there is no significant difference in the levels of receptor molecule expression  
13  
14 for these two conditions (Fig. S13), and thus, the activation of endothelial cells by  
15  
16 chemoattractant must be saturated with 25 ng/mL competing gradients. Accordingly, the  
17  
18 increase in chemoattractant concentration does not enhance adhesion molecule  
19  
20 expression significantly. Based on the results of competing gradients and consideration of  
21  
22 synergistic effects, it is clear that neutrophils prioritize and integrate different  
23  
24 chemoattractant signals simultaneously during the neutrophil TEM process.  
25  
26  
27  
28  
29

## 30 31 **CONCLUSIONS**

32  
33 An *in vivo*-like neutrophil TEM model was fabricated as a microfluidic platform  
34  
35 incorporating a biomimetic hydrogel matrix and a vertical endothelial cell layer to  
36  
37 examine neutrophil migratory responses in various complex microenvironments. We  
38  
39 found that the profiles of single chemical gradients are heavily dependent on the total  
40  
41 concentrations of each chemoattractant, and only the largest concentration (50 ng/mL)  
42  
43 was able to induce significantly more neutrophils moving towards chemoattractant  
44  
45 sources with all considered chemoattractants due to the steepest gradient shapes. In  
46  
47 addition, the single chemoattractant gradient experiments without the cultured endothelial  
48  
49 cell layer reveal that endothelial cells play a crucial role in promoting neutrophil  
50  
51 morphological changes and expression of relevant adhesion molecules. The creation of  
52  
53  
54  
55  
56  
57  
58  
59  
60

1  
2  
3  
4 competing chemoattractant gradients across the hydrogel matrix reveals the hierarchy  
5  
6 among three common neutrophil chemoattractants (fMLP = LTB4 > IL-8), and this order  
7  
8 confirms the previous conclusion that the p38 MAP pathway is dominant over the PI3K  
9  
10 pathway for neutrophil migration, but the introduction of an endothelial cell layer  
11  
12 enhances the ability of LTB4 to promote neutrophil migration. Compared to the  
13  
14 conditions of single chemoattractant gradients, the coexistence of two different  
15  
16 chemoattractants in the same total amount indicate a statistically higher number of cells  
17  
18 migrating into the collagen gel, implying synergistic effects between any two neutrophil  
19  
20 chemoattractants. This is the first time to report competing and synergistic effects among  
21  
22 various chemoattractants in the neutrophil TEM process. In conclusion, this research  
23  
24 describes a promising candidate for neutrophil immunology studies and provides new  
25  
26 insights on the mechanisms of cellular interactions that can be used to predict *in vivo*  
27  
28 neutrophil behaviors during the migration process.  
29  
30  
31  
32  
33  
34  
35  
36  
37

### 38 **ACKNOWLEDGEMENTS**

39  
40  
41 This work was partially supported by a Defense Advanced Research Projects Agency  
42  
43 (DARPA) funding (DARPA 00026142). Device fabrication was done in the Minnesota  
44  
45 Nano Center at University of Minnesota. We would like to thank Dr. Zhe Gao for taking  
46  
47 SEM images of the collagen gel. We also thank the help from Guillermo Marques and  
48  
49 Thomas Pengo in University Imaging Center (University of Minnesota) for recording and  
50  
51 processing confocal images.  
52  
53  
54  
55  
56  
57  
58  
59  
60

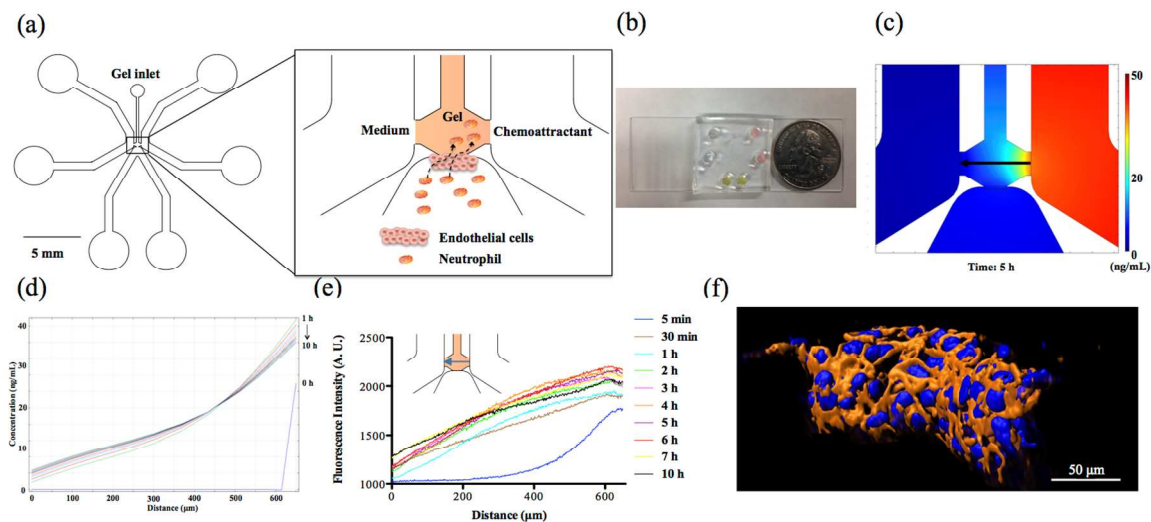


Figure 1. Characterization of neutrophil TEM microfluidic device. (a) Schematic of neutrophil TEM microfluidic device design. Endothelial cells (not to scale) are cultured on the side wall of the collagen gel, and chemoattractant solution or medium is placed in the side channels for developing the chemical gradients. The black arrow line indicates the migration route of neutrophils across the endothelial cell layer towards the chemoattractant source. (b) Photograph of a real device from the top view. (c) COMSOL simulation of a chemical gradient after 5 h diffusion using 50 ng/mL fMLP in the right side channel. The black arrow indicates the direction of gradient from high concentration to low concentration. (d) The COMSOL simulation results of the chemical gradient induced by 50 ng/mL fMLP. (e) The visualization of the fluorescence gradient at the center line of the gel chamber at different time points. (f) Deconvoluted confocal imaging of endothelial cell layer cultured on the side wall of the gel (blue indicates cell nucleus stained by DAPI and orange represents cytoskeletal F-actin labeled by rhodamine phalloidin).



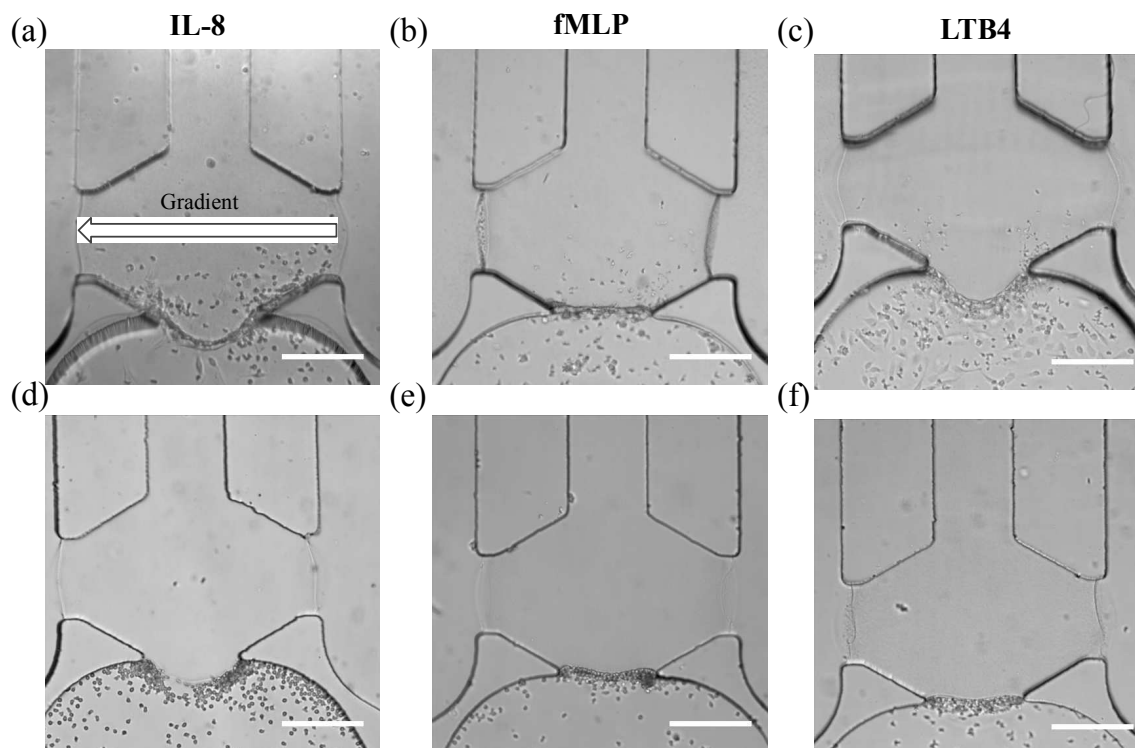


Figure 2. Bright-field images of neutrophil TEM after 5 h neutrophil injection under single chemoattractant gradients (gradient direction is indicated in (a)): (a) 50 ng/mL of IL-8; (b) 50 ng/mL of fMLP; (c) 50 ng/mL of LTB4. Bright-field images of neutrophil migration without an endothelial cell layer after 5 h neutrophil injection under single chemoattractant gradients: (d) 50 ng/mL of IL-8; (e) 50 ng/mL of fMLP; (f) 50 ng/mL of LTB4. Endothelial cells cultured in the bottom channel appear to be in elongated shape (30 ~ 40  $\mu\text{m}$ ) and much larger than the surrounding round neutrophils (~10  $\mu\text{m}$ ). (scale bar: 200  $\mu\text{m}$ )

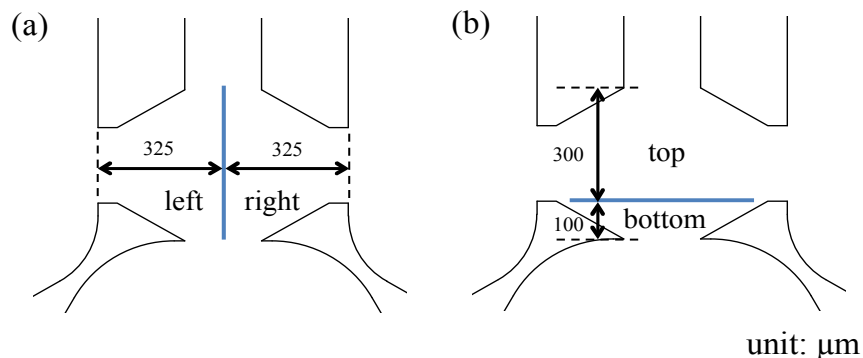


Figure 3. Division of collagen gel chamber into two different parts: (a) left and right parts; (b) top and bottom parts.

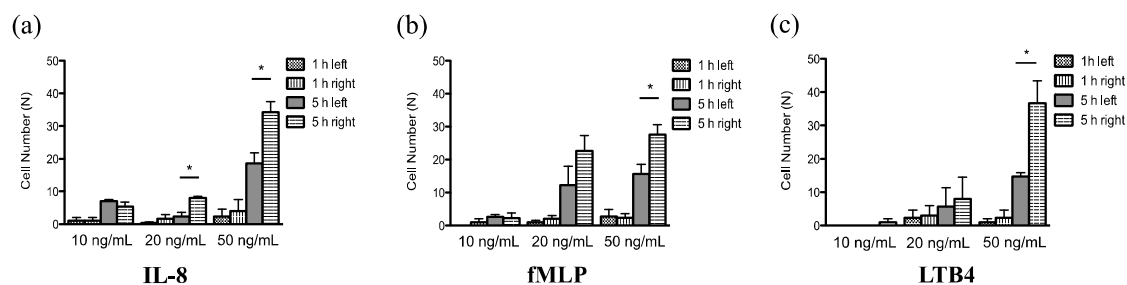


Figure 4. Quantitative analysis of neutrophil TEM after 1 h and 5 h neutrophil injection under various single chemoattractant gradients (\*,  $p < 0.05$ , using a two-tailed unpaired t-test): (a) The number of neutrophils in the left and right parts under (a) 10 ng/mL, 20 ng/mL, and 50 ng/mL of IL-8 gradient; (b) 10 ng/mL, 20 ng/mL, and 50 ng/mL of fMLP gradient; (c) 10 ng/mL, 20 ng/mL, and 50 ng/mL of LTB4 gradient.

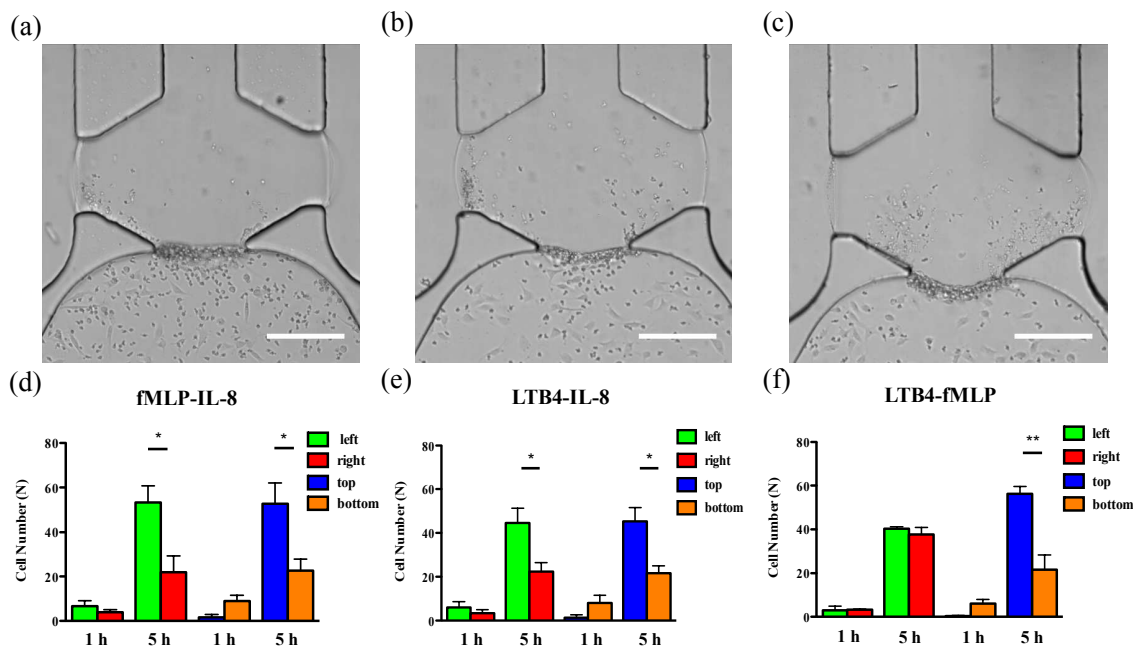


Figure 5. Characterization of neutrophil TEM under competing gradients. Bright-field images of neutrophil TEM 5 h after neutrophil injection (left channel vs. right channel): (a) 50 ng/mL fMLP vs. 50 ng/mL IL-8; (b) 50 ng/mL LTB4 vs. 50 ng/mL IL-8; (c) 50 ng/mL LTB4 vs. 50 ng/mL fMLP. Quantitative analysis of neutrophil numbers in different parts of gel chamber 1 h and 5 h after neutrophil injection: (d) 50 ng/mL fMLP vs. 50 ng/mL IL-8; (e) 50 ng/mL LTB4 vs. 50 ng/mL IL-8; (f) 50 ng/mL LTB4 vs. 50 ng/mL fMLP (\*,  $p < 0.05$ , \*\*,  $p < 0.005$ , using a two-tailed unpaired t-test). Endothelial cells cultured in the bottom channel appear to be in elongated shape (30 ~ 40  $\mu\text{m}$ ) and much larger than the surrounding round neutrophils (~10  $\mu\text{m}$ ). (scale bar: 200  $\mu\text{m}$ )

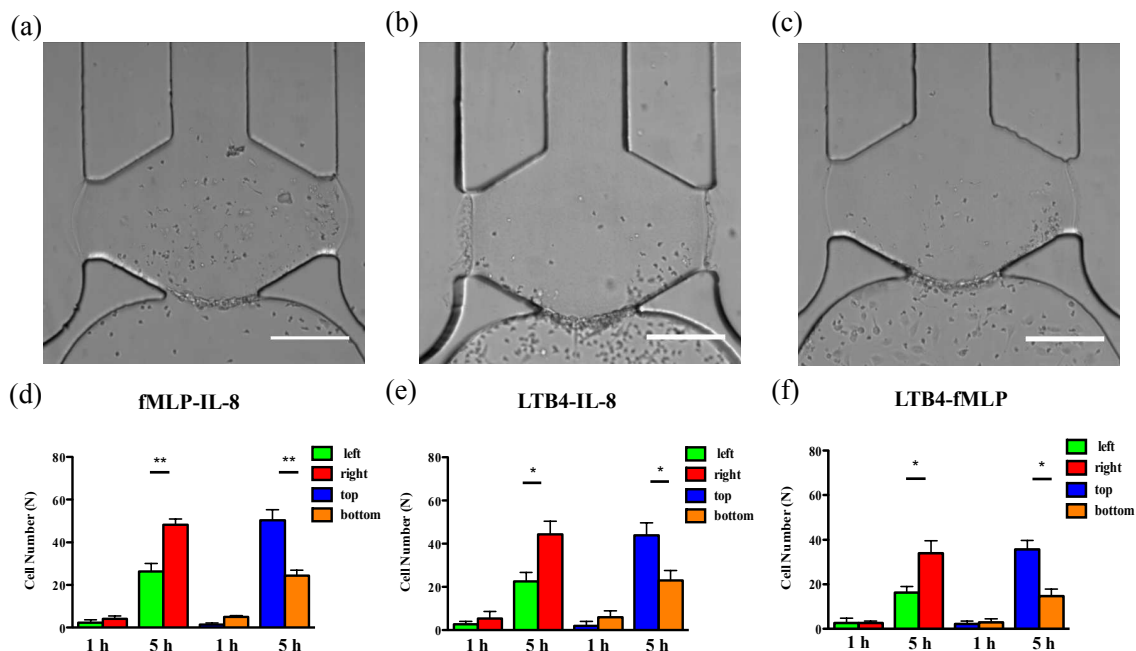


Figure 6. Examination of synergistic effects by mixing two different chemoattractants in the right side channel. Bright-field images of neutrophil TEM 5 h after neutrophil injection: (a) 25 ng/mL fMLP and 25 ng/mL IL-8 in the right channel; (b) 25 ng/mL LTB4 and 25 ng/mL IL-8 in the right channel; (c) 25 ng/mL LTB4 and 25 ng/mL fMLP in the right channel. Quantitative analysis of neutrophil numbers in different parts of the gel chamber 1 h and 5 h after neutrophil injection: (d) 25 ng/mL fMLP and 25 ng/mL IL-8 in the right channel; (e) 25 ng/mL LTB4 and 25 ng/mL IL-8 in the right channel; (f) 25 ng/mL LTB4 and 25 ng/mL fMLP in the right channel (\*,  $p < 0.05$ , \*\*,  $p < 0.005$ , using a two-tailed unpaired t-test). (scale bar: 200  $\mu\text{m}$ )

## References

- (1) B. Amulic, C. Cazalet, G. L. Hayes, K. D. Metzler and A. Zychlinsky, *Ann. Rev. Immunol.*, **2012**, *30*, 459-489.
- (2) E. Kolaczkowska and P. Kubes, *Nat. Rev. Immunol.*, **2013**, *13*, 159-175.
- (3) N. D. Burg and M. H. Pillinger, *Clin. Immunol.*, **2001**, *99*, 7-17.
- (4) H. L. Wright, R. J. Moots, R. C. Bucknall and S. W. Edwards, *Rheumatology*, **2010**, *49*, 1618-1631.
- (5) N. Borregaard, *Immunity*, **2010**, *33*, 657-670.
- (6) J. D. van Buul and P. L. Hordijk, *Arterioscler. Thromb. Vasc. Biol.*, **2004**, *24*, 824-833.
- (7) S. J. Roth, M. W. Carr, S. S. Rose and T. A. Springer, *J. Immunol. Methods*, **1995**, *188*, 97-116.
- (8) Z. Ding, K. Xiong and T. B. J. Issekutz, *Leukoc. Biol.*, **2001**, *69*, 458-466.
- (9) J. Xu, X.-P. Gao, R. Ramchandran, Y.-Y. Zhao, S. M. Vogel and A. B. Malik, *Nat. Immunol.*, **2008**, *9*, 880-886.
- (10) G. M. Whitesides, *Nature*, **2006**, *442*, 368-373.
- (11) S. Chung, R. Sudo, P. J. Mack, C.-R. Wan, V. Vickerman and R. D. Kamm, *Lab Chip*, **2009**, *9*, 269-275.
- (12) G. S. Jeong, S. Han, Y. Shin, G. H. Kwon, R. D. Kamm, S.-H. Lee and S. Chung, *Anal. Chem.*, **2011**, *83*, 8454-8459.
- (13) W. J. Polacheck, J. L. Charest and R. D. Kamm, *Proc. Natl. Acad. Sci. U.S.A.*, **2011**, *108*, 11115-11120.
- (14) M. B. Chen, S. Srigunapalan, A. R. Wheeler and C. A. Simmons, *Lab Chip*, **2013**, *13*, 2591-2598.
- (15) S. Han, J.-J. Yan, Y. Shin, J. J. Jeon, J. Won, H. Eun Jeong, R. D. Kamm, Y.-J. Kim and S. Chung, *Lab Chip*, **2012**, *12*, 3861-3865.
- (16) D. Kim and C. L. Haynes, *Anal. Chem.*, **2013**, *85*, 10787-10796.
- (17) E. K. Sackmann, E. Berthier, E. W. K. Young, M. A. Shelef, S. A. Wernimont, A. Huttenlocher and D. J. Beebe, *Blood*, **2012**, *120*, e45-e53.
- (18) U. Y. Schaff, M. M. Q. Xing, K. K. Lin, N. Pan, N. L. Jeon and S. I. Simon, *Lab Chip*, **2007**, *7*, 448-456.
- (19) R. Snyderman and M. C. Pike, *Ann. Rev. Immunol.*, **1984**, *2*, 257-281.
- (20) C. D. Sadik, N. D. Kim and A. D. Luster, *Trends Immunol.*, **2011**, *32*, 452-460.
- (21) S. E. Van Eeden and T. Terashima, *Leuk. Lymphoma*, **2000**, *37*, 259-271.
- (22) I. A. Reilly, H. R. Knapp and G. A. Fitzgerald, *J. Clin. Pathol.*, **1988**, *41*, 1163-1167.
- (23) S. P. Mathis, V. R. Jala, D. M. Lee and B. Haribabu, *J. Immunol.*, **2010**, *185*, 3049-3056.
- (24) G. Cavicchioni, A. Fraulini, S. Falzarano and S. Spisani, *Eur. J. Med. Chem.*, **2009**, *44*, 4926-4930.

1  
2  
3 (25) F. Pellegatta, Y. Lu, A. Radaelli, M. R. Zocchi, E. Ferrero, S. Chierchia, G. Gaja  
4 and M. E. Ferrero, *Br J. Pharmacol.*, **1996**, *118*, 471-476.

5 (26) F. Pellegatta, S. L. Chierchia and M. R. Zocchi, *J. Biol. Chem.*, **1998**, *273*,  
6 27768-27771.

7 (27) Y. Zheng, J. Chen, M. Craven, N. W. Choi, S. Totorica, A. Diaz-Santana, P.  
8 Kermani, B. Hempstead, C. Fischbach-Teschl, J. A. López and A. D. Stroock, *Proc. Natl.*  
9 *Acad. Sci. U.S.A.*, **2012**, *109*, 9342-9347.

10 (28) H. Oh, B. Siano and S. J. Diamond, *Visualized Exp.*, **2008**, *17*, e745. DOI:  
11 10.3791/745.

12 (29) B. M. Eaton, V. J. Toothill, H. A. Davies, J. D. Pearson, G. E. Mann, *J. Cell.*  
13 *Physiol.* **1991**, *149*, 88-99.

14 (30) M. Dhanabal, R. Ramchandran, M. J. F. Waterman, H. Lu, B. Knebelmann, M.  
15 Segal and V. P. Sukhatme, *J. Biol. Chem.*, **1999**, *274*, 11721-11726.

16 (31) J. Heidemann, H. Ogawa, M. B. Dwinell, P. Rafiee, C. Maaser, H. R. Gockel, M.  
17 F. Otterson, D. M. Ota, N. Lügering, W. Domschke and D. G. Binion, *J. Biol. Chem.*,  
18 **2003**, *278*, 8508-8515.

19 (32) A. Li, S. Dubey, M. L. Varney, B. J. Dave and R. K. Singh, *J. Immunol.*, **2003**, *170*,  
20 3369-3376.

21 (33) K. M. Stroka, H. N. Hayenga and H. Aranda-Espinoza, *H. PLoS ONE*, **2013**, *8*,  
22 e61377.

23 (34) A. R. Burns, R. A. Bowden, S. D. MacDonell, D. C. Walker, T. O. Odebunmi, E.  
24 M. Donnachie, S. I. Simon, M. L. Entman and C. W. J. Smith, *Cell Sci.*, **2000**, *113*, 45-57.

25 (35) S. K. Shaw, P. S. Bamba, B. N. Perkins and F. W. Luscinskas, *J. Immunol.*, **2001**,  
26 *167*, 2323-2330.

27 (36) M. W. J. Boehme, U. Raeth, W. A. Scherbaum, P. R. Galle and W. Stremmel, *Clin*  
28 *& Exp. Immunol.*, **2000**, *119*, 250-254.

29 (37) H. Cho, B. Hamza, E. A. Wong and D. Irimia, *Lab Chip*, **2014**, *14*, 972-978.

30 (38) D. Kim and C. L. Haynes, *Anal. Chem.*, **2012**, *84*, 6070-6078.

31 (39) F. Lin, C.-C. Nguyen, S.-J. Wang, W. Saadi, S. Gross and N. Jeon, *Ann. Biomed.*  
32 *Eng.*, **2005**, *33*, 475-482.

33 (40) B. Heit, L. Liu, P. Colarusso, K. D. Puri and P. Kubes, *J. Cell Sci.*, **2008**, *121*,  
34 205-214.

35 (41) B. Heit, S. M. Robbins, C. M. Downey, Z. Guan, P. Colarusso, B. J. Miller, F. R.  
36 Jirik and P. Kubes, *Nat. Immunol.*, **2008**, *9*, 743-752.

37  
38  
39  
40  
41  
42  
43  
44  
45  
46  
47  
48  
49  
50  
51  
52  
53  
54  
55  
56  
57  
58  
59  
60